JACS
JOURNAL OF THE AMERICAN CHEMICAL SOCIETY

COMMUNICATION

pubs.acs.org/JACS

Revelation of the Molecular Assembly of the Nanoporous Metal Organic Framework ZIF-8

Pak Y. Moh, Pablo Cubillas, Michael W. Anderson, and Martin P. Attfield*

School of Chemistry, The University of Manchester, Oxford Road, Manchester M13 9PL, United Kingdom

Supporting Information

ABSTRACT: Crystalline nanoporous materials are one of the most important families of complex functional material. Many questions pertaining to the molecular assembly mechanism of the framework of these materials remain unanswered. Only recently has it become possible to answer definitively some of these questions by observation of growing nanoscopic surface features on metal organic frameworks (MOFs) through use of *in situ* atomic force microscopy (AFM). Here we reveal that a growth process of a MOF, zeolitic imidazolate framework ZIF-8, occurs through the nucleation and spreading of successive metastable unenclosed substeps to eventually form stable surface steps of the enclosed framework structure and that this process is reliant on the presence of nonframework species to bridge the developing pores during growth. The experiments also enable identification of some of the fundamental units in the growth process and the stable crystal surface plane. The former findings will be applicable to numerous nanoporous materials and support efforts to synthesize and design new frameworks and to control the crystal properties of these materials.

Crystalline nanoporous materials form one of the most important families of functional material that are applied worldwide in a host of applications.[1] The crystal growth of nanoporous materials is different from most other classes of material in that their crystal structures contain structural layers containing the pore or cage volume in which there is no direct bonding between adjacent units of the framework. This poses a variety of questions as to how such parts of the framework develop in the growth stage of crystal growth. Definitive experimental observations to answer such questions can only be achieved through observation of crystal growth at the nanoscale under real-time conditions that has so far remained unreported for any nanoporous material. Here we show that a growth process for a nanoporous metal organic framework (MOF), ZIF-8, occurs through a process of surface nucleation and spreading of successive metastable unenclosed substeps in a correlated manner, and that some of these substeps rely on the presence of nonframework species to provide significant stabilizing interactions to bridge the developing pores of the framework during growth of that particular substep. We also show that the fundamental growth units through which the surface grows are simple species and uniquely determine the stable crystal plane at the crystal surface. Our findings greatly increase the understanding of the synthesis and growth mechanism of MOFs and nanoporous materials that will aid development of improved synthetic strategies to design new frameworks and control their crystal properties, such as, size, habit, composition, and defects, for further application and performance enhancement.

AFM is an ideal technique for making detailed *in situ* observations of nanometer-sized features on growing crystal surfaces to reveal details of the assembly process.[2] MOFs also provide great potential to gain maximum information on such processes for nanoporous materials using AFM as they are often synthesized as single crystals at ambient temperature and pressure, and the framework components, particularly the organic ligand, are relatively large, aiding clear geometric identification.[1] Indeed, the combination of AFM and MOF material has provided a series of images of the stable growth steps and a few single images of the metastable substeps in nonporous and porous MOFs.[3] However, these studies have not yielded more detailed information concerning the actual growth process of the stable growth steps themselves. More detailed information concerning the growth of the stable growth steps can only be determined under conditions for which crystal growth is slow enough to allow longevity of the metastable surface features for detailed observation. Here we use a combination of synthesis protocols and *in situ* AFM to observe the slow growth of nanoporous ZIF-8.

The zinc 2-methylimidazolate [$Zn(C_4H_5N_2)_2$ or $Zn(MeIm)_2$], zeolitic imidazolate framework ZIF-8,[4,5] is a commercially available, highly stable MOF that is receiving great interest for a diverse variety of applications.[6] ZIF-8 is constructed from corner-sharing $Zn(MeIm)_4$ tetrahedral units in which the $MeIm^-$ ligands bridge the Zn^{2+} ions to form a three-dimensional (3D) framework with the sodalite framework topology and a pore size of 3.4 Å (see Figure S1 in the Supporting Information [SI]). Several syntheses of this material has been reported including using dimethylformamide (DMF)[5] or methanol[6b,7] as the solvent. The structural evolution of bulk samples and crystallites of ZIF-8 using a variety of *ex situ* techniques has been reported,[7b] but no detail on the real-time assembly process at the molecular or subnanometer resolution length scale has been reported.

Substrate crystals of ZIF-8 prepared with DMF as the solvent are rhombic dodecahedral in shape with the {110} facets expressed (see Figure S2 [SI]). *In situ* crystal growth of ZIF-8 was observed from a static solution containing 9.8 mL of methanol and 0.20 mL of the solution used to prepare the substrate ZIF-8 crystals that had been heated at 100 °C for three days (see SI for experimental details). AFM deflection micrographs of the (110) face of ZIF-8 are shown in Figures 1 and 2 and Figures S3−S5 in SI. The individual and series of micrographs

Received: June 24, 2011
Published: August 05, 2011

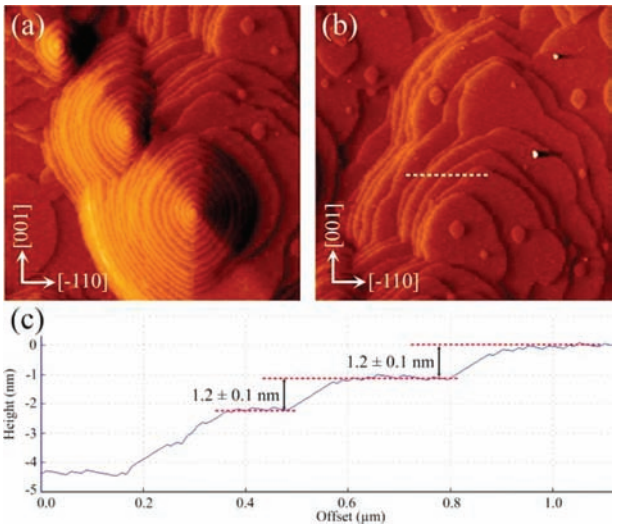

Figure 1. *In situ* AFM deflection images ($4.0 \times 4.0\ \mu m^2$) of the (110) face of ZIF-8 showing growth steps formed by (a) spiral growth mechanism and (b) "birth and spread" mechanism; (c) cross-sectional analyses of some growth steps revealing the 1.2 ± 0.1-nm step heights corresponding to the d_{110} crystal spacing of the material. Dashed white line in (b) indicates the line along which the cross-sectional analysis shown in (c) was performed.

reveal that crystal growth is occurring simultaneously through a "birth and spread" mechanism and a spiral growth mechanism on different regions of the face. This is the first *in situ* observation of spiral growth on a nanoporous MOF material. Attempts to obtain crystal growth from simple methanolic growth solutions of zinc nitrate and 2-methylimidazolate were unsuccessful. The steps of the growth hillocks and spirals exhibit a truncated rhombohedral morphology reflecting the two-fold symmetry of the (110) facets, and the truncated growth in the [−110] direction compared to that in the [001] direction indicates more rapid growth in the latter. Cross-sectional analysis of height images of many of these steps reveals that the majority have heights of 1.2 ± 0.1 nm (see Figures 1c and 2f,g) corresponding to the d_{110} crystal spacing of the structure, as shown in Figure 3a, and reveals strongly preferred surface termination at a well-defined extended structural element.

In situ AFM monitoring of slow crystal growth provides a unique opportunity to observe the nucleation and growth of a stable growth step as shown in the micrographs of Figure 2 and Figures S4 and S5 in SI. Figure 2 shows that a 2D surface nuclei forms on the surface of a growth terrace and subsequently spreads laterally to form a surface growth step. Cross-sectional analysis of the growing step is shown in Figure 2. The height of the step is seen to grow over a time period of 15.6 min with substeps of height 0.4, 0.6, 0.8, 0.9, and 1.1 ± 0.1 nm being observed before the stable extended growth step of 1.2 ± 0.1 nm is formed. The height of the growing step was taken as that recorded at its highest point in each image. Similar series of substep heights of the developing stable extended growth step were observed for five developing nuclei imaged in three independent growth experiments, see Figure S5 in SI for an additional series. This series of height differences uniquely defines the surface crystallographic plane that terminates these stable extended growth steps if it is assumed that the substep heights directly relate to the crystal structure and correspond to

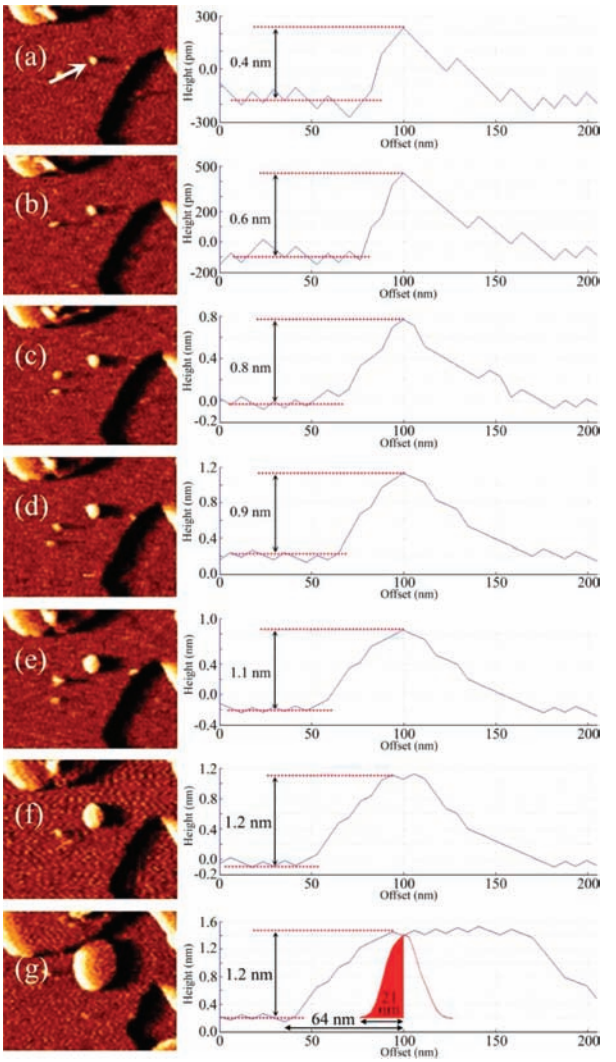

Figure 2. Real-time AFM deflection images and cross-sectional analyses of a developing growth step on the (110) face of a ZIF-8 crystal at 0 (a), 2.9 (b), 4.9 (c), 7.8 (d), 12.8 (e), 15.6 (f), and 40 (g) min after first observation of the 2D surface nuclei. (g) Cross-sectional profiles and lateral dimensions of a typical step edge and the AFM tip. Cross-sectional profiles were taken in directions parallel to the fast scan direction that is parallel to the horizontal edge of the images. The nucleus for which growth is being monitored is highlighted by the white arrow in (a). Image sizes are all $0.5 \times 0.4\ \mu m^2$.

the differences in height between different solvated Zn^{2+} ions and the uppermost nitrogen atoms of solvated $MeIm^-$ ions. This demonstrates the use of *in situ* AFM to determine experimentally the crystallographic surface plane of a complex material. The surface plane is that formed by the layer of Q^3 Zn^{2+} ions at (X) in Figure 3a (where Q^3 indicates that the Zn^{2+} ion is only bound into the bulk crystal structure by 3 out of 4 possible linkers) and leaves the least number of bonding sites per Zn species unintegrated into the bulk crystal structure.

Comparison of the observed substep heights and the plausible height differences in the crystal structure provides a wealth of information concerning the growth process. Addition of a $MeIm^-$ unit to a surface Q^3 Zn^{2+} ion results in a height difference of 0.4 nm, as shown in Figure 3a and SI Figure S6, which is in excellent agreement with the 0.4 nm observed substep height.

dx.doi.org/10.1021/ja205900f |*J. Am. Chem. Soc.* 2011, 133, 13304–13307

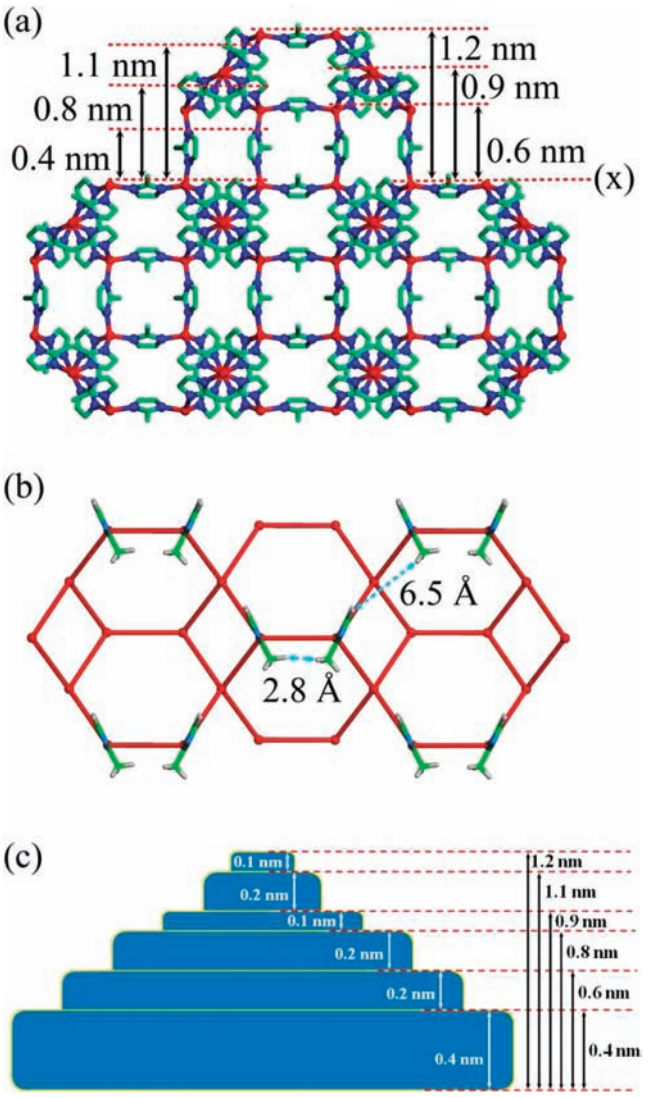

Figure 3. (a) Structure of ZIF-8 viewed along the [100] direction highlighting the heights of the metastable substeps through which the structurally enclosed stable 1.2-nm high growth step is formed; (b) view along the [110] direction highlighting the spatial separation of the developing vertical sides of the 4-/6-rings on the (110) facet with the closest hydrogen−hydrogen distances marked; (c) schematic of the formation of the stabilized 1.2-nm high growth step by the incremental nucleation and spreading of subsequent metastable unenclosed substeps. The heights of the substeps in (c) relative to the terrace of the most immediate underlying substep and the respective underlying stabilized extended step are shown. The structures in (a) and (b) are represented in ball-and-stick mode: red = Zn, blue = N, green = C. For clarity, H atoms have been omitted from (a), and $MeIm^-$ ligands have been omitted from the base layer of the structure in (b).

This result has major implications concerning the crystal growth mechanism of this material. It first implies that the terminating species on a Q^3 Zn^{2+} ion is not a $MeIm^-$ ion but rather a more weakly coordinated solvent or other species. This provides direct information to the surface termination of the Q^3 Zn^{2+} ion in a ZIF material under growth conditions, information that has been provided currently for ZIF-8 by computational methods predominantly.[8] Second, the fact that a surface nucleation has grown in a correlated manner into a surface growth step has important ramifications in relation to the understanding of the growth of framework and nanoporous solids. To form a metastable substep of height 0.4 nm indicates that $MeIm^-$ ions attached to the surface must influence the attachment of incoming $MeIm^-$ ions adjacent to themselves. The shortest H···H interatomic distances between $MeIm^-$ ions are 2.8 and 6.5 Å, across the materializing 4- and 6-rings of the structure respectively as shown in Figure 3b. This implies that a $MeIm^-$ ion must interact with additional species, presumably the solvent molecules, and induce a degree of ordering of these molecules to allow the formation of a continuous substep in a correlated fashion that spans the distances involved in forming the rings, particularly the 6-rings, of the structure. This continuously connected 0.4-nm high substep contains no strong coordinate bonds in directions parallel to the crystal surface. No direct evidence for the presence of the localized solvent molecules in the formation of the 6-ring is apparent from the AFM data; however, some *a posteri* confirmation for this interaction may be derived from the single-crystal structure of as-synthesized ZIF-8[5] in which electron density assigned to disordered solvent molecules is found above the center of the 6-ring with distances from the center of the electron density to the hydrogen atoms of the $MeIm^-$ groups of 3.1 Å. This result demonstrates definitively that this framework solid is reliant on the presence of nonframework species to provide significant stabilizing interactions to bridge the pores of the framework during crystal growth and that even the relatively weak solvent−framework dispersive or hydrogen-bond interactions are strong enough for the necessary local ordering to occur to achieve growth of the cages of this nanoporous material.

The next observed substep height is 0.6 nm which in terms of the crystal structure corresponds to the addition of further Zn^{2+} and $MeIm^-$ ions to the surface-tethered $MeIm^-$ ions to complete the substep of 4-rings, see Figures 3a and S6 (SI). The observed height of 0.6 nm implies that solvated $[(-MeIm)_2Zn(solvent)_n]^+$ ions terminate this substep of 4-rings and not $[(-MeIm)_2Zn(MeIm)_2]^-$. Observation of the 0.4- and 0.6-nm high substeps provides a strong indication that crystal growth involves direct addition of simple monomeric $MeIm^-$ and solvated Zn^{2+} ion species and not larger clusters or secondary building units, such as $[Zn(MeIm)_4]^{2-}$ species. This result demonstrates that ZIF-8 synthesis, like other carboxylate-based MOFs, involves solely simple monomeric species, and not larger, preformed, secondary building units.[3c,9,10]

The final observed substep heights of 0.8, 0.9, and 1.1 nm correspond to the addition of further $MeIm^-$ and Zn^{2+} ions to the 0.6-nm high substep. Consideration of the plausible height differences in the crystal structure indicates that addition of subsequent $MeIm^-$ and Zn^{2+} species to the 0.6-nm high substep would provide substep heights of 0.75/0.84 (0.8), 0.9, 1.08/1.16 (1.1), 1.2 nm as shown in Figures 3a and S6 (SI). This indicates the step continues to grow through further direct addition of simple monomeric $MeIm^-$ and solvated Zn^{2+} ion species until the enclosed framework structure of the 1.2-nm high stabilized growth step is formed. Some of the finer detail of the latter substeps formed from addition of the $MeIm^-$ ions is not possible to resolve because the height differences are so small.

The lateral resolution obtained through AFM imaging is an order of magnitude less than the vertical resolution due, in part, to the observed cross-sectional profile of any step edge being a convolution of the AFM tip shape and the actual structure of the step edge being imaged. However, cross-sectional analyses of the step edges do provide insight into the growth mechanism.

dx.doi.org/10.1021/ja205900f |*J. Am. Chem. Soc.* 2011, 133, 13304–13307

Cross-sectional analyses of several edges of 1.2-nm high stabilized growth steps of different areas reveal the lateral dimension of the step edge to be 70(6) nm, as shown in Figure 2g. Cross-sectional analyses of sharp 1.2-nm high growth features on the surface of zeolite-L, used as a calibrant,[11] imaged under liquid conditions using the same type of tip reveal the lateral dimension of the tip shape to be 22(2) nm, as shown in Figure 2g. The differences in cross-sectional profiles and lateral dimensions indicate that the cross-sectional profile of the 1.2-nm high stabilized growth step edges is far less steep than that of the tip shape alone and rises in a more gradual manner from zero to 1.2 nm above the terrace surface below.

The aforementioned results suggest that the 1.2-nm high stabilized growth steps grow through a process of nucleation and spreading, in a correlated manner, of metastable unenclosed substeps as shown schematically in Figure 3c. The cross-sectional profile and lateral dimension of several step edges of 1.2-nm high stabilized growth steps of different area, from diameters of 200 nm to 3 μm, remain approximately constant. This, in addition to the extended longevity of the surface plane that is formed by the layer of Q^3 Zn^{2+} ions at (X) in Figure 3a, indicates that the process of nucleation and spreading of the 0.4-nm high substep is rate limiting and that the rates of lateral spreading of all the subsequent substeps within the 1.2-nm high stabilized growth step are approximately similar.

Obtaining similar mechanistic information concerning the development of a growth spiral is far more difficult owing to the limited number of spirals that are observed during growth and the difficulties in imaging and analyzing accurately the core of the developing spiral. However, cross-sectional analyses of the edge of the 1.2-nm high stabilized step of a growing spiral reveal the lateral dimension of the step edge to be 71(10) nm, which is in good agreement with the value obtained from the growth steps formed by the "birth and spread" mechanism. This provides some indication that the 1.2-nm high stabilized spiral growth step develops through the spreading, in a correlated manner, of metastable unenclosed substeps in a manner similar to that of the 2D surface growth steps.

In conclusion, this work provides the first definitive evidence that the framework, encompassing void volume, in a nanoporous material can be formed through a process of nucleation and spreading, in a correlated manner, of metastable unenclosed substeps to eventually form stable surface steps of the enclosed framework structure and that this process is reliant on the presence of nonframework species to provide the stabilizing interactions to bridge the developing pores during crystal growth. The work also identifies simple monomeric species as the fundamental growth species in this process and determines the stable crystal surface plane of ZIF-8. Although this study has involved a MOF material solely, this general mechanism of growth occurring through the nucleation and spreading of successive metastable unenclosed substeps to form stable surface steps of the enclosed framework structure is likely to be applicable to the growth of numerous members of the family of nanoporous or framework material and will create greater understanding of their synthesis, leading to more considered approaches to the formation and control of the framework structure and overall crystal properties of these materials.

■ ASSOCIATED CONTENT

Supporting Information. Full experimental details, SEM and AFM micrographs and images of the crystal. This material is available free of charge via the Internet at http://pubs.acs.org.

■ AUTHOR INFORMATION

Corresponding Author
m.attfield@manchester.ac.uk

■ ACKNOWLEDGMENT

We acknowledge the EPSRC and the Leverhulme Trust for funding and the Malaysian government for provision of a studentship for P.Y.M.

■ REFERENCES

(1) (a) Wright, P. A. *Microporous Framework Solids*; RSC: Cambridge, 2008. (b) Ferey, G. *Chem. Soc. Rev.* **2008**, *37*, 191–214. (c) Rowsell, J. L. C.; Yaghi, O. M. *Microporous Mesoporous Mater.* **2004**, *73*, 3–14. (d) Kitagawa, S.; Kitaura, R; Noro, S. *Angew. Chem., Int. Ed.* **2004**, *43*, 2334–2375. (e) Rosseinsky, M. J. *Microporous Mesoporous Mater.* **2004**, *73*, 15–30.

(2) (a) McPherson, A.; Malkin, A. J.; Kuznetsov, Y. G. *Annu. Rev. Biophys. Biomol. Struct.* **2000**, *29*, 361–410. (b) Weaver, M. L.; Qiu, S. R.; Friddle, R. W.; Casey, W. H.; De Yoreo, J. J. *Cryst. Growth Des.* **2010**, *10*, 2954–2959. (c) Sethmann, I.; Wang, J.; Becker, U.; Putnis, A. *Cryst. Growth Des.* **2010**, *10*, 4319–4326.

(3) (a) Carlucci, L.; Ciani, G.; Moret, M.; Proserpio, D. M.; Rizzato, S. *Chem. Mater.* **2002**, *14*, 12–16. (b) Moret, M.; Rizzato, S. *Cryst. Growth Des.* **2009**, *9*, 5035–5042. (c) Shöâeè, M.; Anderson, M. W.; Attfield, M. P. *Angew. Chem., Int. Ed.* **2008**, *47*, 8525–8529. (d) John, N. S.; Scherb, C.; Shoaee, M.; Anderson, M. W.; Attfield, M. P.; Bein, T. *Chem. Commun.* **2009**, 6294–6296.

(4) Huang, X.-C.; Lin, Y.-Y.; Zhang, J.-P.; Chen, X.-M. *Angew. Chem., Int. Ed.* **2006**, *45*, 1557–1559.

(5) Park, K. S.; Ni, Z.; Cote, A. P.; Choi, J. Y.; Huang, R. D.; Uribe-Romo, F. J.; Chae, H. K.; O'Keeffe, M.; Yaghi, O. M. *Proc. Nat. Acad. Sci. U.S.A.* **2006**, *103*, 10186–10191.

(6) (a) Chang, N.; Gu, Z. Y.; Yan, X. P. *J. Am. Chem. Soc.* **2010**, *132*, 13645–13647. (b) Lu, G.; Hupp, J. T. *J. Am. Chem. Soc.* **2010**, *132*, 7832–7833. (c) Venna, S. R.; Carreon, M. A. *J. Am. Chem. Soc.* **2010**, *132*, 76–78. (d) Jiang, H.-L.; Liu, B.; Akita, T.; Haruta, M.; Sakurai, H.; Xu, Q. *J. Am. Chem. Soc.* **2009**, *131*, 11302–11303.

(7) (a) Cravillon, J.; Munzer, S.; Lohmeier, S.-J.; Feldhoff, A; Huber, K.; Wiebcke, M. *Chem. Mater.* **2009**, *21*, 1410–1412. (b) Venna, S. R.; Jasinski, J. B.; Carreon, M. A. *J. Am. Chem. Soc.* **2010**, *132*, 18030–18033.

(8) (a) Chizallet, C.; Lazare, S.; Bazer-Bachi, D.; Bonnier, F.; Lecocq, V.; Soyer, E.; Quoineaud, A. A.; Bats, N. *J. Am. Chem. Soc.* **2010**, *132*, 12365–12377. (b) Chizallet, C.; Bats, N. *J. Phys. Chem. Lett.* **2010**, *1*, 349–353.

(9) (a) Shekhah, O.; Wang, H.; Kowarik, S.; Schreiber, F.; Paulus, M.; Tolan, M.; Sternemann, C.; Evers, F.; Zacher, D.; Fischer, R. A.; Woll, C. *J. Am. Chem. Soc.* **2007**, *129*, 15118–15119. (b) Shekhah, O.; Wang, H.; Zacher, D.; Fischer, R. A.; Woll, C. *Angew. Chem., Int. Ed.* **2009**, *48*, 5038–5041. (c) Shekhah, O.; Wang, H.; Paradinas, M.; Ocal, C.; Schüpbach, B.; Terfor, A.; Zacher, D.; Fischer, R. A.; Woll, C. *Nat. Mater.* **2009**, *8*, 481–484.

(10) (a) Surble, S.; Milange, F.; Serre, C.; Ferey, G.; Walton, R. J. *Chem. Commun.* **2006**, 1518–1520. (b) Rood, J. A.; Boggess, W. C.; Noll, B. C.; Henderson, K. W. *J. Am. Chem. Soc.* **2007**, *129*, 13675–13682.

(11) Brent, R.; Anderson, M. W. *Angew. Chem., Int. Ed.* **2008**, *47*, 1–5.